A Preliminary Tectonic Fabric Chart of the Indian Ocean

JEAN-YVES ROYER[1], JOHN G. SCLATER[1,2] AND DAVID T. SANDWELL[1]

[1] Institute for Geophysics
The University of Texas at Austin
8701 MOPAC Blvd, Austin, TX 78759-8345

[2] Department of Geological Sciences
The University of Texas at Austin
P.O. Box 7346, Austin, TX 78713-7346

Abstract

We present a preliminary tectonic chart of the Indian Ocean based on a joint compilation of bathymetric data, magnetic anomaly data and Geosat altimetry data. Satellite altimeters such as Geosat map the topography of the equipotential sea surface or marine geoid. Our interpretation of the data Geosat data is based on an analysis of the first derivative of the geoid profiles (i.e. deflection of the vertical profiles). Because of the high correlation between the vertical deflection (at wavelength < 200 km) and the seafloor topography, the Geosat profiles can be used to delineate accurately numerous tectonic features of the ocean floor such as fracture zones, seamounts and spreading ridges. The lineations in the Geosat data are compared with bathymetric data and combined with magnetic anomaly identifications to produce a tectonic fabric chart of the Indian Ocean floor.

Keywords: Indian Ocean, Geosat altimeter, deflection of the vertical, tectonic fabric chart.

1. Introduction

In the past few years, as a result of development of remote sensing and data imaging techniques, better resolution and coverage have permitted the upgrading of the tectonic picture of the ocean floor. In the Indian Ocean, one may examine the development of this improved resolution by comparing the successive tectonic charts produced by Heezen and Tharp (1965) and Udintsev et al. (1975), and the bathymetric charts of the GEBCO series (1975-1982) with the recent chart of the gravity field by Haxby (1985). Satellite altimeters (GEOS-3, SEASAT, GEOSAT) map the topography of the equipotential sea surface (marine geoid). Due to the uniform coverage of the satellite ground tracks and the excellent correlation between the short wavelengths (20-200 km) of the geoid signal with the topographic gradient of the ocean floor, the satellite altimeter data bring a wealth of rigorously comparable information bearing on the morphology of the seafloor, especially in the remote inhospitable and hence poorly charted southern oceans. There, in particular, previously unrecognized tectonic elements, specifically fracture zones and seamounts, have been delineated or verified (e.g., Haxby, 1985; Lazarewicz and Schwank, 1982; Sandwell, 1984; Sandwell and McAdoo, 1988).

Recently, Gahagan et al. (1988) have used the anomalies and lineations in plots of the deflection of the vertical from SEASAT data to portray a preliminary fabric chart of the ocean floor. In this paper, we expand upon this approach by presenting first, plots of the actual deflection of the vertical data along tracks, second, identifying lineations in these plots and finally, third, comparing these lineations with bathymetric features and magnetic anomaly

Proceedings of the Indian Academy of Sciences, James N. Brune (Editor), in press.

identifications in order to construct a preliminary tectonic fabric map of the ocean floor. This work is based primarily on the GEOSAT data which we combine with the SEASAT data set. This analysis reveals new features on the seafloor at the southerly latitudes that are related to the early phase evolution of the Indian Ocean. Recently-refined portrayals of tectonic fabrics of the seafloor provide exceptionally good constraints for plate tectonic reconstructions far beyond those available to the pioneer modelers of the evolution of the Indian Ocean (e.g., Fisher et al., 1971; McKenzie and Sclater, 1971; Sclater and Fisher, 1974; Norton and Sclater; 1979; Patriat, 1987). In fact, problems with previous reconstruction models have generally arisen in areas where either the fracture zone lineations or the magnetic lineations were poorly established trough lack of shipborne coverage. Hence, the joint compilation of magnetic anomalies and fracture zone lineations from closely-spaced altimetry traverses has proved to be a very powerful approach as it allows us to revise and improve our understanding of the tectonic history of the ocean floor (e.g., Royer et al., 1988; Royer and Sandwell, 1989; Mayes et al., 1989).

2. A Tectonic History of the Indian Ocean

The Indian Ocean floor (Fig. 1) is characterized by a system of three active spreading ridges that now separates four major fragments of the former supercontinent Gondwana: Africa, India, Australia and Antarctica. The northern branch of this ridge system rises in the Gulf of Aden, separating Africa from Arabia, and continues along the Carlsberg Ridge and the Central Indian Ridge which separates Africa from India. At 25°S, 70°E, the Central Indian Ridge intersects the two other branches, the Southwest Indian Ridge that extends between Africa and Antarctica towards the South Atlantic, and the Southeast Indian Ridge that extends towards the South Pacific between Antarctica and India, and Antarctica and Australia. Numerous ridges and plateaus of intermediate depth, which may be taken to characterize the Indian Ocean, appear on either sides of the spreading ridges. The size, number and distribution of these elevations have raised many questions about their nature and origin as well as their role in the continuing development of the Indian Ocean. From east to west, they are the South Tasman Rise, the plateaus off western Australia (Naturaliste, Cuvier, Wallaby, Exmouth), Broken Ridge and the Kerguelen Plateau, Ninetyeast Ridge, Chagos-Laccadive Ridge and the Mascarene Plateau, the Chain and Murray Ridges, Madagascar Plateau, Del Cano Rise, Crozet Plateau, Conrad Rise, Gunnerus Ridge, Mozambique Ridge, Astrid Ridge, Agulhas Plateau and finally Maud Rise (Fig. 1).

According to interpretations of the seafloor magnetic anomaly pattern as identified in the Indian Ocean, the major basins lying between the spreading ridges, the continental margins and the submarine ridges evolved during three main periods. From the breakup of Gondwana in the Late Jurassic to the midCretaceous, Africa separated from Madagascar and Antarctica, creating respectively the western Somali Basin (Ségoufin and Patriat, 1980; Rabinowitz et al., 1983; Coffin and Rabinowitz, 1987; Cochran, 1988), the symmetric Mozambique Basin (Ségoufin, 1978; Simpson et al., 1979) and the basin off Dronning Maud Land, Antarctica (Bergh, 1977, 1987). During the same time period, India and Madagascar separated from Australia and Antarctica, creating the Mesozoic basins along the western margin of Australia (Markl, 1974, 1978; Larson et al., 1979; Veevers et al., 1985). From the midCretaceous to the Middle Eocene, the major motion resulted in the rapid northward drift of India towards Asia. Most of the floor of the Indian Ocean was created during this phase: the basins between Africa-Madagascar and Antarctica (Bergh and Norton, 1976; Patriat, 1979, LaBrecque and Hayes, 1979; Sclater et al., 1981; Fisher and Sclater, 1983), the Madagascar and the Mascarene Basins, the eastern Somali Basin and the Arabian Sea between Africa-Madagascar and India (McKenzie and Sclater, 1971; Whitmarsh, 1974; Schlich, 1975, 1982), the mirrored Central Indian Basin and Crozet Basin between India and Antarctica (McKenzie and Sclater, 1971; Sclater and Fisher, 1974; Schlich, 1975, 1982) and the Wharton Basin between India and

Australia (Sclater and Fisher, 1974; Liu et al., 1983). In addition, during this period, Australia and Antarctica commenced to separate (Cande and Mutter, 1982). The latest period in the evolution of the Indian Ocean started with a major reorganization of the spreading centers, consequent to the collision of India with Asia in the Middle Eocene. Seafloor spreading ceased in the Wharton Basin while major changes in the direction and rate of spreading occurred in the Central Indian Basin, the Crozet Basin, the Madagascar Basin, the eastern Somali Basin and the Arabian Sea. The new configuration of the spreading ridges corresponds to the present-day ridge system. During this phase, the Australian-Antarctic Basin (Weissel and Hayes, 1972), the southern Central Indian Basin (Sclater et al., 1976a) and the northern Crozet Basin (Schlich, 1975) were created. Also, the Mascarene Plateau and the Chagos-Laccadive Ridge separated (Fisher et al., 1971; McKenzie and Sclater, 1971), and the Gulf of Aden opened (Laughton et al., 1970). Because of the differential motion along the Central Indian Ridge and the Southeast Indian Ridge, the Southwest Indian Ridge propagated rapidly towards the east (Tapscott et al., 1980; Sclater et al., 1981; Patriat, 1987).

3. Analysis of the Altimetry Data: Lineations in the Deflection of the Vertical Charts

The SEASAT satellite, launched by NASA in 1978, used a radar altimeter to make precise measurements (Tapley et al., 1982) of the sea-surface or geoid height (~ 0.1 m) over most of the world's oceans. Unfortunately, the SEASAT mission failed after a few months, and almost no data were recovered from the areas south of 62°S because of the ice-coverage around Antarctica at the time that SEASAT operated. In March 1985, the US Navy launched the GEOSAT altimeter in order to map the marine geoid to a high spatial resolution on a global basis. Only the data from the Exact Repeat Mission, started in November 1987, which duplicated the 17 days SEASAT repeat orbits, have yet been unclassified. However, because the ground track spacing (~ 164 km at the Equator) decreases at the high latitudes, and because GEOSAT operated during the Austral ice-free summer, the information from the high southerly latitudes, between 60°S and 72°S, is exceptionally good. In this study, we use mainly the GEOSAT data. The accuracy is about 3 times better than for the SEASAT (Sandwell and McAdoo, 1988) and we improve this accuracy and data recovery along tracks by stacking 22 GEOSAT repeat cycles. For wavelengths greater than 20 km, the RMS noise level of the GEOSAT data is about 1 to 2 mGals. However, in order to take advantage of the better density of the SEASAT data north of 60°S, we combine both SEASAT and GEOSAT data sets when the amplitudes of the SEASAT signal were above the noise level.

To enhance the short wavelengths of the marine geoid signal, it is more appropriate to use the deflection of the vertical that is the first derivative of the gravity along the track. Deflection of the vertical, expressed in microradians, measures the variation of the horizontal gravity field. One microradian (μrad) is roughly equivalent to an horizontal variation in gravity of one milligal (mGal). Figures 2 and 3 display the deflection of the vertical plotted along respectively the descending and ascending satellite ground tracks. Vertical bars along tracks are spaced every 4 data points (~ 14 km apart). Amplitudes are positive to the north. The scale of amplitude is 20 μrad/degree of longitude; however when greater than 30 μrad, the amplitudes are reduced through an Arctg function. Long wavelength (> 4000 km) and short wavelength noise (< 20 km) have been removed, after stacking, from each pass using the procedure described by Sandwell and McAdoo (1988).

Figure 4A through 4J display a series of different interpretation of the deflection of the vertical signal. In a tectonic fabric chart, we are mostly interested in the lineated features such as fracture zones, spreading ridges, linear troughs, ridges or plateaus, and trenches. Depending on their extension, most of these features have a reproducible signature on a set of parallel profiles, which make them easy to identify. The signature of a fracture zone will vary

according to the spreading rate and the age offset (Fig. 4A and 4B). Depending on the direction of the satellite and the orientation of the tectonic feature relative to the satellite ground track, the signature of a tectonic feature can be identical or reversed on the ascending or descending data sets. As a rule of thumb, topographic features oriented north-south will have same signatures; in the case of a fracture zone (Fig. 4C), both the ascending and descending profiles cross the topographic (age) offset from the same side. East-west oriented features will have reversed signatures; in Figure 4D, ascending and descending profiles approach the fracture zone from opposite sides. Because the age offset reverses at the midpoint of the transform segment of a fracture zone, the signature of a fracture zone is symmetric relative to the fracture zone axis and of opposite sign on either side of this point (Fig. 4E). Finally, the spacing of parallel fracture zones is also an important factor; the combined effects of parallel topographic (age) offsets may produce a large signal where the signal produced by each individual fracture zone cannot be identified (e.g., Prince Edward FZ area along the Southwest Indian Ridge). The signature of a spreading ridge axis depends on the spreading rates as does the topography (Fig. 4F and 4G). Seamounts have a typical signature (Fig. 4H) recognizable at isolated, sharp and narrow positive and negative picks of equal amplitude. Trenches (Fig. 4I) are characterized by a succession of positive and negative picks related to the flexure of the lithosphere ahead of the trench and to the trench itself. Continental rise (Fig. 4J) and linear offsets in the oceanic basement are also clearly identifiable. Finally, aseismic ridges and plateaus are clearly visible, but, depending on their width and height relative to the adjacent basins, they are difficult to chart. The deflection of the vertical charts of the Indian Ocean (Fig. 2 and 3) provide examples for each type of feature. We have traced lineations in these charts by correlating respectively peaks and troughs (i.e., steepest horizontal gradient of the gravity) in the deflection of the vertical plots, on both the ascending and descending passes. Figure 5 summarizes our interpretation of the lineations in the deflection of the vertical plots. We have abbreviated the name of this chart to deflection of the vertical lineations. Symbols show the actual location of the data points and lines, the lineations. We deliberately have not represented the peaks and troughs associated with large topographic features of the ocean floor, outlined on Figure 5 by bathymetric contours. Such features are better represented by direct contouring of the gravity field (e.g., Haxby, 1985).

4. Tectonic Fabric Chart of the Indian Ocean

The deflection of the vertical plots amplify the short wavelength of the geoid. Lineations in these charts are in general related to high amplitude short wavelength topographic features such as transform faults, fracture zones, seamounts and other discrete entities on the seafloor. By combining the lineations of the deflection of the vertical charts with transform faults and fracture zones known from topographic and magnetic surveys, it is possible to create an improved tectonic chart of the sea floor. Because of the greater coverage of the satellite data and the ability of the presentation to amplify and extend lineated features both above and below sediment, the resultant signal presents a fabric chart of the igneous basement of the seafloor. We have abbreviated the name of these combined charts to "tectonic fabric charts".

The lineations in the deflection of the vertical charts (Fig. 5) are documented to varying degree depending on the characteristics of seafloor spreading in the oceanic basins: spreading rate, paleo-direction of spreading relative to the satellite ground tracks and the age offsets across the fracture zones. The interpretation of the deflection of the vertical charts brings new information mainly on the southerly latitudes around Antarctica regarding the early phase of seafloor spreading between Africa and Antarctica during the Late Jurassic up to the Late Cretaceous, and between Antarctica and Australia during the Middle Eocene. In addition, due to the uniform coverage of the satellite profiles, the fracture zones are generally better sampled and their pattern better defined on the deflection of the vertical charts than on

tectonic charts based on shipborne data. This is for instance the case along the Central Indian Ridge, or between Broken Ridge and the Kerguelen Plateau, or between Tasmania and Antarctica. Except for this latter area, most of the fracture zones in the Indian Ocean are oblique or perpendicular to the ascending satellite tracks and parallel or sub-parallel to the descending tracks. Therefore, they are more visible on the ascending passes (Fig. 3) than on the descending passes (Fig. 2), while the opposite occurs for the Indian Ocean spreading ridges. However, in some areas such as the Australian-Antarctic Discordance where the fracture zones are oriented north-south and the ridge axes east-west, both data sets are complementary.

In regard to the evolution of the Indian Ocean, the best documented period corresponds to the latest and most recent phase of seafloor spreading that started after the general reorganization of the plate boundaries in the Middle Eocene. Along the Sheba, Carlsberg and Central Indian Ridges, the fracture zones strike N50°E to N60°E. From the northwest to the southeast, the main fracture zones are the Alula-Fartak FZ (13°N, 51°E) at the mouth of the Gulf of Aden, the Owen FZ (12°N, 56°E) separating the Sheba Ridge from the Carlsberg Ridge, the fracture zone at 3°N, the Mahabiss FZ (3°S), the Sealark FZ (4°S), the Vitiaz FZ (8°S), the Vema FZ (11°S), the Argo FZ (14°S), the Marie Celeste FZ (17°S) and the Egeria FZ (20°S) which lies east of the Rodrigues Ridge. Except for the Alula-Fartak FZ and the fracture zone at 3°N, all the ridge offsets are right-lateral. The largest transform offsets are located along the Alula-Fartak FZ (200 km), the Owen FZ (300 km), the Vema FZ (200 km) and the Marie Celeste FZ (220 km). Along the Southwest Indian Ridge, the orientation of the fracture zones varies progressively from N45°E in the vicinity of the Bouvet Triple Junction (55°S, 1°W) to north-south, west of the Indian Ocean triple junction (25°S, 70°E). From west to east, they are Bouvet FZ (2°E), Moshesh FZ (5°E), Islas Orcadas FZ (6°E), Shaka FZ associated with the Shaka Ridge (8°E), Dingaan FZ (12°E), Mandela FZ (15°E), Du Toit FZ (26°E), the Andrew Bain FZ complex (28°E), Prince Edward FZ (35°E), Discovery II FZ (43°E), Indomed FZ (46°E), Gallieni FZ (52°E), the Atlantis II FZ (58°E) and the Melville FZ (61°E). The ridge offsets are left-lateral and generally important (100 to 200 km) for all these fracture zones; the major offset (800 km) along the Southwest Indian Ridge axis occurs between Bain FZ and Prince Edward FZ (28°E to 35°E). Finally, along the Southeast Indian Ridge, the fracture zone trends, oriented N45°E in the vicinity of the Indian Ocean triple junction, shift progressively to N15°E-N10°E between Australia and Antarctica, and reach N15°W in the vicinity of the Macquarie triple junction (61°S, 162°E). The major offsets are located along the Amsterdam and St Paul FZ (78°E) and along the George V, Tasman and Balleny FZ. The fracture zone pattern between Australia and Antarctica, particularly the prominent fracture zones south of Tasmania that can be traced all the way south into the Antarctic margin, tightly constrain the reconstructions in the Australian-Antarctic Basin since the Middle Eocene (Anomaly 20). Prior to that time and since the initiation of spreading in the Late Cretaceous, seafloor spreading was extremely slow (0.5 cm/a; Cande and Mutter, 1982) and the magnetic lineations are continuous and parallel to the Australian and Antarctic margins.

The spacing between satellite profiles is generally too large (160-80 km) to allow an accurate mapping of the mid-oceanic ridge axes. Though in several areas, the deflection of the vertical data show an excellent correlation with the location of the ridge axes deduced from bathymetric and magnetic data. The Sheba Ridge is characterized by a slow spreading rate (1 cm/a, Laughton et al., 1970) and an axial valley that deepens towards the east. The ridge axis produces a clear signature on the deflection of the vertical signal, as illustrated on Figure 4G, that defines two continuous ridge segments separated by the Alula-Fartak FZ. The Carlsberg Ridge has similar characteristics as the Sheba Ridge with spreading rate ranging from 1.2 to 1.3 cm/a (Le Pichon and Heirtzler, 1968; McKenzie and Sclater, 1971) and shows a linear and nearly continuous ridge axis from the Owen FZ to the Equator. The Central Indian Ridge, which runs between the Mascarene

Plateau and the Chagos-Laccadive Ridge, is extremely segmented by closely spaced fracture zones. The first ridge segments clearly identifiable out of the geoid signal caused by the fracture zones are located southeast of the Rodrigues Ridge. The spreading rates for this mid-oceanic ridge range from north to south between 1.8 and 2.4 cm/a (Fisher et al., 1971; Patriat, 1987). The Southwest Indian Ridge has a very slow spreading rate (less than 1 cm/a; Schlich and Patriat, 1971a; Sclater et al., 1976b; Sclater et al., 1981; Patriat, 1987) and is expressed by a deep and pronounced inner valley. Several extensive ridge segments are well delineated by the deflection of the vertical data between the Mandela and Du Toit FZ which is the longest segment, east of the Prince Edward FZ, between the Discovery II, Indomed, and Gallieni FZ, and between the Melville FZ and the Indian Ocean triple junction. The Southeast Indian Ridge is the most active of the three Indian mid-oceanic ridges with medium spreading rates increasing from west to east from 3.0 to 3.5 cm/a (Schlich and Patriat, 1971b; Weissel and Hayes, 1972; Schlich, 1975; Patriat, 1987). Between the Indian Ocean triple junction and the Amsterdam and St Paul FZ, the ridge axis is segmented by several fracture zones and is generally well expressed by an axial valley, while east of the St Paul FZ the ridge segments are long and continuous and expressed by a central rise, typical for medium or fast spreading ridges (Weissel and Hayes, 1972; Royer and Schlich, 1988). The area of the Australian-Antarctic Discordance presents an anomalous topography and fracture zone pattern (Vogt et al., 1983). The deflection of the vertical signal along the Southeast Indian Ridge varies from that of Figure 4F and 4G. The trenches along the Java and Sumatra Islands and south of New Zealand are the second type of present-day plate boundaries that clearly show on the deflection of the vertical data.

The altimetry data add little information on the fabric of the oceanic basins related to the second phase of opening of the Indian Ocean, from the mid-Cretaceous to the Middle Eocene. Only the Murray Ridge and the Chain Ridge, on either sides of the Owen Fracture Zone, document in the Arabian Sea and eastern Somali Basin the drift of India away from the Seychelles and East Africa. The structural directions in the Central Indian Basin and the Wharton Basin (McKenzie and Sclater, 1971; Sclater and Fisher, 1974), which record the fast northward drift of India relative to Antarctica and Australia, do not show well on the deflection of the vertical data. Their north-south orientation is too close from those of the satellite profiles. In the Wharton Basin, in addition to the Investigator FZ and the eastern scarp of the Ninetyeast Ridge, a cross grain is apparent, while intraplate deformation within the Central Indian Basin cause east-west undulation of the lithosphere that obliterate and obscure the tectonic fabrics (e.g., Weissel et al., 1980; Geller et al., 1983; Haxby, 1985; McAdoo and Sandwell, 1985). However, in the conjugate basins, the Madagascar and Crozet Basins, the fracture zone pattern is well recognizable. The most important feature is the Kerguelen Fracture Zone that offset the magnetic lineations 32, 33 and 34 (Schlich, 1982; Patriat, 1987) by more than 800 km. With the GEOSAT data, it becomes clear that this feature does not extend further south than 62°S, and therefore post-dates the plate boundary reorganization in the mid-Cretaceous. In the Mascarene Basin, part of the extinct spreading system is visible. This system initiated at the time of the break-up between India and Madagascar in the mid-Cretaceous and died in the Paleocene/Early Eocene (chron 31 to 27; Schlich, 1982) when the spreading ridge jumped to the north to form the Carlsberg Ridge and subsequently separated India from the Seychelles and the northern Mascarene Plateau. Remnant of the fossil spreading axis can be identified southwest of La Réunion Island (La Réunion Trench), north of the Mauritius Trench extension that forms the limit of the extinct spreading system with the Madagascar Basin. The fossil spreading ridge is offset 400 km to the north by the Mahanoro FZ and Wilshaw Ridge complex. Further north, the fracture zone pattern becomes unclear. Finally, the most interesting information related to mid-Cretaceous/Middle Eocene time span concerns the relative motion of Africa and Antarctica. A clear set of parallel fracture zones can be defined

between the Agulhas Plateau and the Maud Rise and Astrid Ridge, off Antarctica. At 48°S on the northern flank, and at 58°S, on the southern flank, there is a clear disruption of the fracture zone pattern which is shifted, by 50 to 100 km, to the east or to the west, respectively. This demonstrates the change of motion that occurred in the Paleocene (anomaly 31 to 24; Larson et al. 1985; Patriat et al., 1985; Royer et al., 1988). This change of motion is particularly well recorded by the large offset northeast of Astrid Ridge (~40 Ma age offset). Such a change of motion will also match perfectly the extremities of the fracture zones lying immediately west of the Madagascar Plateau (northern flank) and Conrad Rise (southern flank). The Prince Edward FZ is therefore a recent feature (Middle Eocene, chron 20) and is not the continuation of the fracture zone running from Astrid Ridge.

Finally, new evidence about the early phase of opening of the Indian Ocean, from the Late Jurassic to the mid-Cretaceous, are found in the western part of the Enderby Basin. East of the fracture zone near Astrid Ridge, several parallel fracture zones are delineated in the deflection of the vertical charts. It shows that the direction of motion between Africa and Antarctica remained the same for 34 Ma, from chron M0 (118 Ma) identified east of the Astrid Ridge (Bergh, 1977, 1987) to chron 34 (84 Ma) located west of Conrad Rise (Bergh and Norton, 1976; Patriat et al., 1985). To the north, except for the Davie Ridge that records the relative motion between Africa and Madagascar, no fracture zone shows on the deflection of the vertical data: neither in the Mozambique Basin (Ségoufin, 1978; Simpson et al., 1979), nor in the western Somali Basin (Ségoufin and Patriat, 1981; Rabinowitz et al., 1983) or off the east African margin (Bunce and Molnar, 1977; Cochran, 1988). This due to their north south orientation and to the very important thickness of sediments in these old basins. Along the western Australian margins, only the large offset Investigator FZ, the scarps of the Wallaby and Cuvier Plateaus, and the Naturaliste FZ that abuts the Naturaliste Plateau are visible. The possible curvature of the Investigator FZ into the Wallaby and Cuvier Plateau would be a direct evidence of the mid-Cretaceous oceanwide change in the plate motions.

Some linear and continuous features, not related to directions of relative motion, produce a typical signature on the horizontal gravity field. Among the most spectacular are the conjugate escarpments of Broken Ridge and the Kerguelen Plateau. These lines correspond to an offset of the basement along the Kerguelen Plateau (Coffin et al., 1986) and to a deep linear trough along Broken Ridge (Fisher et al., 1982). According to Mammerickx and Sandwell (1986), these topographic features are related to the demise of seafloor spreading in the Wharton Basin (Liu et al., 1983; Geller et al., 1983) and the initiation of spreading between the two plateaus (Mutter and Cande, 1983) at chron 18-19 (~45 Ma). The match of these two curves provides a tight constraint upon the relative position of the Kerguelen Plateau and Broken Ridge prior to their break-up. The continent/ocean boundary mapped along the southern margin of Australia from magnetic and seismic evidence (Talwani et al., 1979; Konig, 1980; Veevers, 1986) has a distinct and characteristic deflection of the vertical signature. We have used this criteria to identify the conjugate boundary along the Antarctic margin where the data are very limited. The deflection of the vertical signature also clearly outlines the limit of the continental shelf break (steepest gradient of the horizontal gravity field). Generally, this structural limit is well mapped from bathymetric data; however, around Antarctica where the data are sparse and scattered because of the remoteness and the ice-coverage, the altimery data now permit to delineate accurately the limit of the continental plateau. Another clearly visible feature is the change of topographic grain between the crust created along the Southwest Indian Ridge (at a slow spreading rate) and the crust created along the Southeast Indian Ridge and the Central Indian Ridge (at medium spreading rates). Actually, the age of this limit decreases towards the east, demonstrating the eastward propagation of the Southwest Indian Ridge (Patriat, 1979; Tapscott et al., 1980; Sclater et al., 1981). Patriat (1987) mapped independently these two limits

as the traces of the Indian Ocean triple junction respectively on the African and Antarctic plates.

5. Conclusion: a revised tectonic summary diagram for the Indian Ocean

Comparison of bathymetric data, deflection of the vertical lineations, and magnetic anomaly data permits the construction of a revised tectonic fabric chart for the Indian Ocean (Fig. 6). This chart is of significant value especially in the far southern ocean where new fracture zones have been identified and previously charted fracture zones extended. However, it is still only preliminary in nature as we have neither integrated the deflection of the vertical data with the actual topographic data to produce improved topographic charts (e.g., Driscoll et al., unpublished manuscript, 1986) or repicked any magnetic anomalies. In addition, the geoid or gravity field of the oceans (Haxby, 1985) contains very valuable information on the origin and structure of broad basic features of the ocean floor. This present study is the first step of an international attempt to integrate all the above information, to provide some useful preliminary constraints for studies of the Indian Ocean tectonic history, and to show what can be accomplished by such integrated approach.

For the sake of clarity, we did not represent in Figure 6 all the magnetic lineations that have been identified in the Indian Ocean; in particular for the Cenozoic, we have selected chron 34, 33, 31, 28, 24, 20, 18, 13, 6 and 5. The wealth of data accumulated in the Indian Ocean now represents as many constraints as one must reconcile in a consistent plate kinematic model. There are still some areas where data are lacking, for instance, south of the Kerguelen Plateau in the Enderby Basin, in the vicinity of the Ninetyeast Ridge, in the Bengal Fan, in the Arabian Sea beneath the Indus Fan, in the region bounded by Chain Ridge, the Seychelles, the Mesozoic fracture zones in the western Somali Basin, and the adjacent Mascarene Basin. These areas mainly concern the mid-Cretaceous times when the plate boundaries reorganized (Cretaceous Quiet Zone). For this reason, no satisfactory model has yet been proposed to link consistently all the Mesozoic basins in the Indian Ocean, the South Atlantic and the Weddell Sea.

Acknowledgments. This work is part of a joint cooperative program between the Institut de Physique du Globe de Strasbourg, the Institute for Geophysics at U.T. Austin (UTIG), the Lamont Doherty Geological Observatory, and the Scripps Institution of Oceanography. The authors wish to thank Robert L. Fisher for constructive comments on the manuscript. Help from Lisa Gahagan in completing the figures is greatly appreciated. This work was supported by NSF Grant OCE-86 17193 and by the sponsors of the Paleoceanographic Mapping Project (POMP) at the Institute for Geophysics, the University of Texas at Austin. UTIG contribution 767.

References

Bergh, H. W., 1977: Mesozoic seafloor off Dronning Maud Land, Antarctica. *Nature*, 269: 686-687.

Bergh, H. W., 1987: Underlying fracture zone nature of Astrid Ridge off Antarctica's Queen Maud Land. *J. Geophys. Res.*, 92: 475-484.

Bergh, H. W., and Norton, I. O., 1976: Prince Edward fracture zone and the evolution of the Mozambique Basin. *J. Geophys. Res.*, 81: 5221-5239.

Bunce, E. T., and Molnar, P., 1977: Seismic reflection profiling and basement topography in the Somali Basin: possible fracture zones between Madagascar and Africa. *J. Geophys. Res.*, 82: 5305-5311.

Cande, S. C., and Mutter, J. C., 1982: A revised identification of the oldest sea-floor spreading anomalies between Australia and Antarctica. *Earth Planet. Sci. Lett.*, 58: 151-160.

Cochran, J., 1988: The Somali Basin, Chain Ridge and the origin of the northern Somali Basin gravity and geoid low. *J. Geophys. Res.*, 93: 11985-12008.

Coffin, M. F., and Rabinowitz, P. D., 1987: Reconstruction of Madagascar and Africa: evidence from the Davie Fracture Zone and western Somali Basin *J. Geophys. Res.*, 92: 9385-9406.

Coffin, M. F., Davies, H. L., and Haxby, W. F., 1986: Structure of the Kerguelen Plateau province from SEASAT altimetry and seismic reflection data. *Nature*, 324: 134-136.

Driscoll, M. L., Fisher, R. L., and Parsons, B., 1986: Fracture zone trends and structure of the Souhtwest Indian Ridge: an investigation using Seasat

altimetry and surface-ship bathymetry. *Unpublished manuscript.*

Falconer, R. H. K., and Tharp, M., 1982: General Bathymetric Chart of the Oceans (GEBCO), sheet 5•14. Canadian Hydrographic Service, Ottawa, Canada.

Fisher, R. L., Sclater, J. G., and McKenzie, D. P., 1971: Evolution of the Central Indian Ridge. *Geol. Soc. Amer. Bull.*, 82: 553-562.

Fisher, R.L., Jantsch, M. Z., and Comer, R. L., 1982: General Bathymetric Chart of the Oceans (GEBCO), sheet 5•9. Canadian Hydrographic Service, Ottawa, Canada.

Fisher, R. L., and Sclater, J. G., 1983: Tectonic evolution of the Southwest Indian Ridge since the mid-Cretaceous: plate motions and stability of the pole of Antarctica/Africa for at least 80 Ma. *Geophys. J. R. astr. Soc.*, 73: 553-576.

Gahagan, L. M., Royer, J.-Y., Scotese, C. R., Sandwell, D. T., Winn, K., Tomlins, R.L., Ross, M. I., Newman, J. S., Müller, D., Mayes, C. L., Lawver, L. A., and Huebeck, C. E., 1988: Tectonic fabric map of the ocean basins from satellite altimetry data. In Scotese, C. R., and W. W. Sager (Eds), Mesozoic and Cenozoic plate reconstructions, *Tectonophysics*, 155: 1-26.

Geller, C. A., Weissel, J. K., and Anderson, R. N., 1983: Heat transfer and intraplate deformation in the central Indian Ocean. *J. Geophys. Res.*, 88: 1018-32.

Haxby, W. F., 1985: Gravity field of World's Oceans (color map). Lamont Doherty Geological Observatory of Columbia University, Palisades, NY.

Hayes, D. E., and Vogel, M., 1981: General Bathymetric Chart of the Oceans (GEBCO), sheet 5•13. Canadian Hydrographic Service, Ottawa, Canada.

Heezen, B. C., and Tharp, M., 1965: Physiographic diagram of the Indian Ocean (with descriptive sheet). *Geol. Soc. Am. Inc.*, New-York, NY.

König, M., 1980: Geophysical investigations of the southern continental margin of Australia and the conjugate sector of East Antarctica. PhD. Thesis, Columbia University, New-York, NY, 337p.

LaBrecque, J. L., and Hayes, D. E., 1979: Seafloor spreading history of the Agulhas Basin. *Earth Planet. Sci. Lett.*, 45: 411-428.

LaBrecque, J. L., and Rabinowitz, P. D., 1981: General Bathymetric Chart of the Ocean (GEBCO), sheet 5•16. Canadian Hydrographic Service, Ottawa, Canada.

Larson, R.L., Mutter, J.C., Diebold, J.B., and Carpenter G.B., 1979: Cuvier Basin: a product of ocean crust formation by Early Cretaceous rifting off Western Australia. *Earth. Planet. Sci. Lett.*, 45: 105-114.

Larson, R.L., Pitman, W.C., Golovchenko, X., Cande, S.C., Dewey, J.F., Haxby, W.F., and LaBrecque, J.L., 1985: The Bedrock Geology of the World (color map), Freeman and Co, New-York, NY.

Laughton, A. S., Whitmarsh, R. B., and Jones, M. T., 1970: The evolution of the Gulf of Aden. *Phil. Trans. Roy. Soc. London*, A-267: 227-266.

Laughton, A. S., 1975: General Bathymetric Chart of the Oceans (GEBCO), sheet 5•5. Canadian Hydrographic Service, Ottawa, Canada.

Lazarewicz, A. R., and Schwank, D. C., 1982: Detection of uncharted seamounts using satellite altimetry. *Geophys. Res. Lett.*, 9: 385-388.

Le Pichon, X., and Heirtzler, J.R., 1968: Magnetic anomalies in the Indian Ocean and sea-floor spreading. *J. Geophys. Res.*, 73: 2101-2117.

Liu, C.S., Curray, J.R., and Mc Donald, J.M., 1983: New constraints on the tectonic evolution of the Eastern Indian Ocean. *Earth Planet. Sci. Lett.*, 65: 331-342.

McAdoo, D. C., and Sandwell, D. T., 1985: Folding of the oceanic lithosphere. *J. Geophys. Res.*, 90: 8563-8569.

McKenzie, D. P., and Sclater, J. G., 1971: The evolution of the Indian Ocean since the Late Cretaceous. *Geophys. J. R. astr. Soc.*, 25: 437-528.

Mammerickx, J., and Sandwell, D. T., 1986: Rifting of old oceanic lithosphere. *J. Geophys. Res.*, 91: 1975-88.

Markl, R.G., 1974: Evidence for the breakup of Eastern Gondwanaland by the Early Cretaceous. *Nature*, 251: 196-200.

Markl, R.G., 1978: Further evidence for the Early Cretaceous breakup of Gondwanaland off Southwestern Australia. *Marine Geol.*, 26: 41-48.

Mayes, C. M., Sandwell, D. T., and Lawver, L. A., 1989: Tectonic history and new isochron chart of the South Pacific. *J. Geophys. Res.*, in press.

Monahan, D., Falconer, R.H., and Tharp, M., 1982: General Bathymetric Chart of the Oceans (GEBCO), sheet 5•10. Canadian Hydrographic Service, Ottawa, Canada.

Mutter, J.C., and Cande, S.C., 1983: The early opening between Broken Ridge and Kerguelen Plateau. *Earth Planet. Sci. Lett.*, 65: 369-376.

Norton, I. O., and Sclater, J. G., 1979: A model for the evolution of the Indian Ocean and the breakup of Gondwanaland. *J. Geophys. Res.*, 84, 6803-6830.

Patriat, P., 1979: L'océan Indien occidental: la dorsale ouest-indienne. *Mém. Mus. Nat. Hist. Nat.*, 43: 49-52.

Patriat, P., 1987: Reconstitution de l'évolution du système de dorsales de l'océan Indien par les méthodes de la cinématique des plaques. Publ. by Territoire des Terres Australes et Antarctiques Françaises, Paris, 308p.

Patriat, P., Ségoufin, J., Goslin, J., and Beuzart, P., 1985: Relative positions of Africa and Antarctica in the Upper Cretaceous: evidence for a non-stationary behaviour of fracture zones. *Earth Planet. Sci. Lett.*, 75: 204-214.

Rabinowitz, P. D., Coffin, M. F., and Falvey, D., 1983: The separation of Madagascar and Africa. *Science*, 220: 67-69.

Royer, J.-Y., Patriat, P., Bergh, H., and Scotese, C.R., 1988: Evolution of the Southwest Indian Ridge from the Late Cretaceous (anomaly 34) to the Middle Eocene (anomaly 20). In Scotese, C. R., and W. W. Sager (Eds), Mesozoic and Cenozoic plate reconstructions, *Tectonophysics*, 155: 235-260.

Royer, J.-Y., and Schlich, R., 1988: The Southeast Indian Ridge between the Rodriguez Triple Junction and the Amsterdam and Saint-Paul Islands: detailed kinematics for the past 20 Ma. *J. Geophys. Res.*, 93: 13524-13550.

Royer, J.-Y., and Sandwell, D. T., 1989: Evolution of the eastern Indian Ocean since the Late Cretaceous: Constraints from GEOSAT altimetry. *J. Geophys. Res.*, in press.

Sandwell, D. T., 1984: A detailed view of the South Pacific geoid from satellite altimetry. *J. Geophys. Res.*, 89: 1089-1104.

Sandwell, D.T., and Mc Adoo, D.C., 1988: Marine gravity of the Southern Ocean and Antarctic Margin from GEOSAT: tectonic implications. *J. Geophys. Res.*, 93: 10389-10396.

Schlich, R., 1975: Structure et âge de l'océan Indien occidental. *Mém. hors série Soc. Geol. France*, 6: 103 pp.

Schlich, R., 1982: The Indian Ocean: aseismic ridges, spreading centers and basins. In: A. E. Nairn and F. G. Stheli (eds), *The Ocean Basins and Margins*: the Indian Ocean, Plenum Press, New-York, 6: 51-147.

Schlich, R., and Patriat, P., 1971a: Mise en évidence d'anomalies magnétiques axiales sur la banche ouest de la dorsale médio-indienne. *C. R. Acad. Sci. Paris*, 272(D): 700-703.

Schlich, R., and Patriat, P., 1971b: Anomalies magnétiques de la branche est de la dorsale médio-indienne entre les îles Amsterdam et Kerguelen. *C. R. Acad. Sci. Paris*, 272(B): 773-776.

Schlich, R. , Coffin, M. F., Munschy, M., Stagg, H. M. J., Li, Z. G., and Revill, K., 1987: Bathymetric chart of the Kerguelen Plateau. Joint publication of the Bureau of Mineral Resource, Canberra, Australia, and the Institut de Physique du Globe, Strasbourg, France.

Sclater, J. G., and Fisher, R. L., 1974: Evolution of the east-central Indian Ocean, with emphasis on the tectonic setting of the Ninetyeast Ridge. *Geol. Soc. Am. Bull.*, 85: 683-702.

Sclater, J.G., Luyendyk, B.P., and Meinke, L., 1976a: Magnetic lineations in the Southern part of the Central Indian Basin. *Geol. Soc. Am. Bull.*, 87: 371-378.

Sclater, J. G., Bowin, C., Hey, R., Hoskins, H., Peirce, J., Philipps, J., and Tapscott, C., 1976b: The Bouvet triple junction. *J. Geophys. Res.*, 81: 1857-1869.

Sclater, J. G., Fisher, R. L., Patriat, P., Tapscott, C., and Parsons, B., 1981: Eocene to recent development of the Southwest Indian Ridge, a consequence of the evolution of the Indian Ocean triple junction. *Geophys. J. R. astr. Soc.*, 64: 587-604.

Ségoufin, J., 1978: Anomalies magnétiques mésozoïques dans le bassin de Mozambique. *C. R. Ac. Sci.*, 287: 109-112.

Ségoufin, J., and Patriat, P., 1980: Existence d'anomalies mésozoïques dans le bassin de Somalie. Implications pour les relations Afrique-Antarctique-Madagascar. *C. R. Acad. Sci. Paris*, 291(B): 85-88.

Ségoufin, J., and Patriat, P., 1981: Reconstructionns de l'océan Indien occidental pour les époques des anomalies M21, M2 et 34. Paléoposition de Madagascar. *Bull. Soc. Géol. France*, 23: 693-707.

Simpson, E. S. W., Sclater, J. G., Parsons, B., Norton, I. O., and Meinke, L., 1979: Mesozoic magnetic lineations in the Mozambique Basin. *Earth Planet. Sci. Lett.*, 43: 260-264.

Talwani, M., Mutter, J., Houtz, R., and König, M., 1979: The crustal structure and evolution of the area underlying the magnetic quiet zone on the margin south of Australia. In: Watkins, Montadert and Dickerson (eds), Geological and geophysical investigations of the continental margins. *Am. Assoc. Pet. Geol. Mem.*, 29: 151-175.

Tapley, B. D., Born, G. H., and Park, M. E. 1982: The SEASAT alimeter data and its accuracy assessment. *J. Geophys. Res.*, 87: 3179-3188.

Tapscott, C., Patriat, P., Fisher, R. L., Sclater, J. G., Hoskins, H., and Parsons, B., 1980: The Indian Ocean triple junction. *J. Geophys. Res.*, 85: 4723-4739.

Udintsev, G. B., Fisher, R. L., Kanaev, V.F., Laughton, A. S., Simpson, E. S. W., and Zhiv, D. I., 1975: Geological-geophysical atlas of the Indian Ocean. Academy of Sciences of the U.S.S.R., Moscow, 151p.

Veevers, J.J., 1986: Breakup of Australai and Antarctica estimated as mid-Cretaceous (95±5 Ma) from magnetic and seismic data at the continental margin. *Earth Planet. Sci. Lett.*, 77: 91-99.

Veevers, J.J., Tayton, J. W., Johnson, B.D., and Hansen, L., 1985: Magnetic expression of the continent-ocean boundary between the western margin of Australia and the Eastern Indian Ocean. *J. Geophys.*, 56: 106-120.

Vogt, P. R., Cherkis, N. Z., and Morgan, G. A., 1983: Project Investigator I: evolution of the Australia-Antarctic discordance deduced from a detailed aeromagnetic survey. In: Antarctic Earth Science, R. L. Oliver, P. R. James and J. B. Lago (eds): Proceeding of the IV International Symposium on Antarctic Earth Science, Australian Academy Press, Canberra: 608-613.

Weissel, J.K., and Hayes, D.E., 1972: Magnetic anomalies in the Southeast Indian Ocean. In: Antarctic Oceanology II: The Australain-New Zealand sector, D.E. Hayes (ed.), *Am. Geophys. Un. Ant. res. Ser.*, 19: 165-196.

Weissel, J.K., Anderson, R.N., and Geller, C.A., 1980: Deformation of the Indo-Australian plate. *Nature*, 287: 284-291.

Whitmarsh, R. B., 1974: Some aspects of plate tectonics in the Arabian Sea. In: *Initial reports of the Deep Sea Drilling Project*, 23: 527-535.

Figure Captions

Figure 1: Chart index of geographical names of the Indian Ocean (redrawn from Laughton, 1975; Hayes and Vogel, 1981; LaBrecque and Rabinowitz, 1981; Falconer and Tharp, 1982; Fisher et al., 1982; Monahan et al., 1982; Schlich et al., 1987).

Figure 2: GEOSAT descending profiles of the deflection of the vertical plotted along the satellite ground tracks. Positive is to the north.

Figure 3: GEOSAT ascending profiles of the deflection of the vertical plotted along the satellite ground tracks. Positive is to the north.

Figure 4: Schematic signatures of the geoid and the deflection of the vertical (horizontal derivative of the gravity field) across some tectonic features of the ocean floor:
A), B) Fracture zones. Since the deflection of the vertical is the horizontal derivative of the geoid along the satellite ground track, the sign of the signal changes with the direction of the satellite.
C), D) Deflection of the vertical plotted at right angle of the subsatellite tracks. Positive is to the north (top of page). Descending and ascending profiles will have an identical signature across a north-south oriented fracture zone, while they will show an opposite signature across an east-west oriented fracture zone.
E) Variation of the deflection of the vertical signal along a fracture zone (same convention as for C and D). The signal reverses at the midpoint of the transform segment of the fracture zone as does the age offset.
F), G) Deflection of the vertical signature above spreading ridge axes.
H) Seamount signatures generally show two sharp positive and negative picks of equal amplitude.
H) Trench
J) Continental rise

Figure 5: Lineations in the deflection of the vertical profiles (i.e., horizontal variation of the gravity field).

Figure 6: Tectonic summary chart of the Indian Ocean resulting from the combined compilation of interpretations of magnetic anomaly data, bathymetric data and deflection of the vertical profiles (same scale as GEBCO chart 5•00).

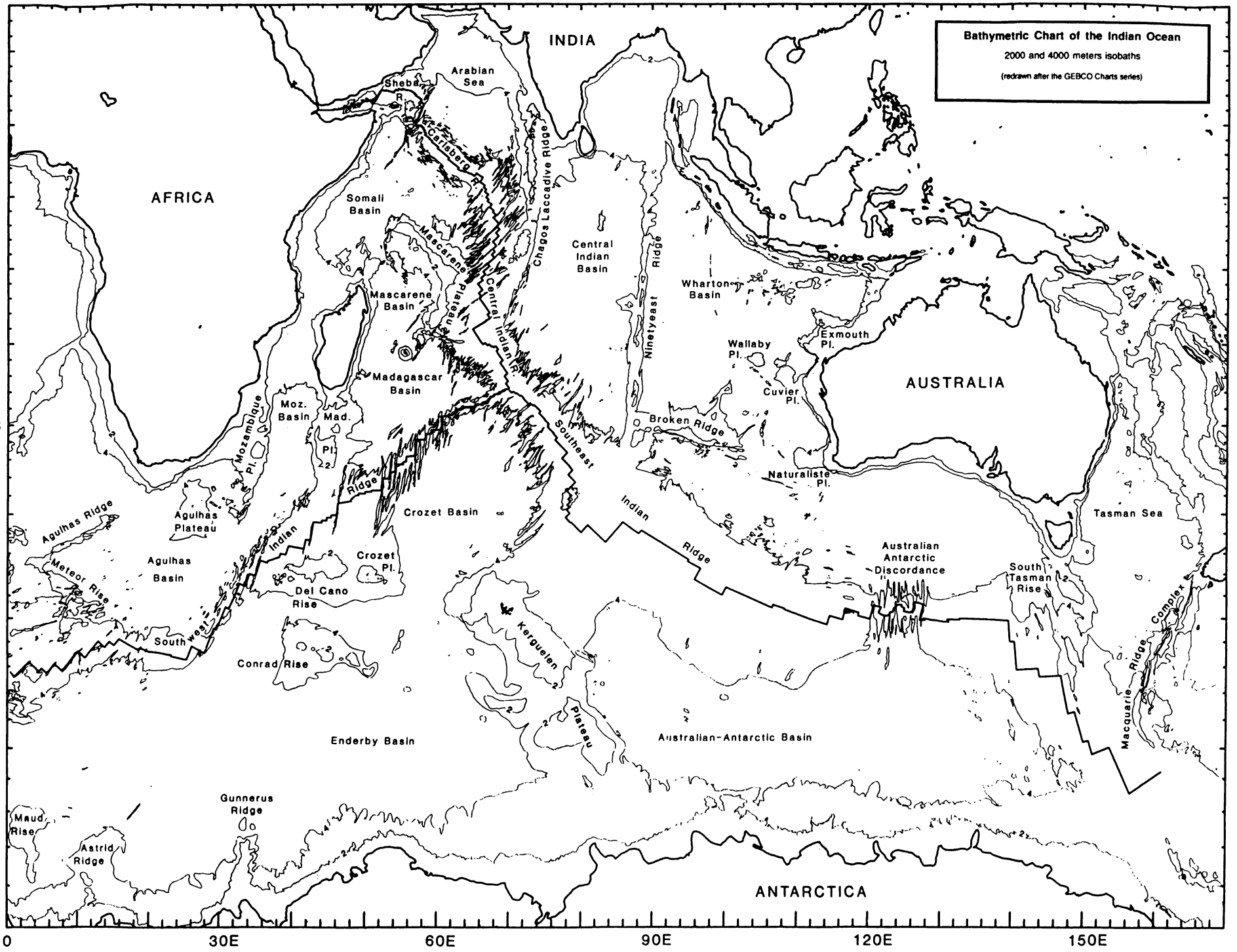

Figure 1

Figure 1

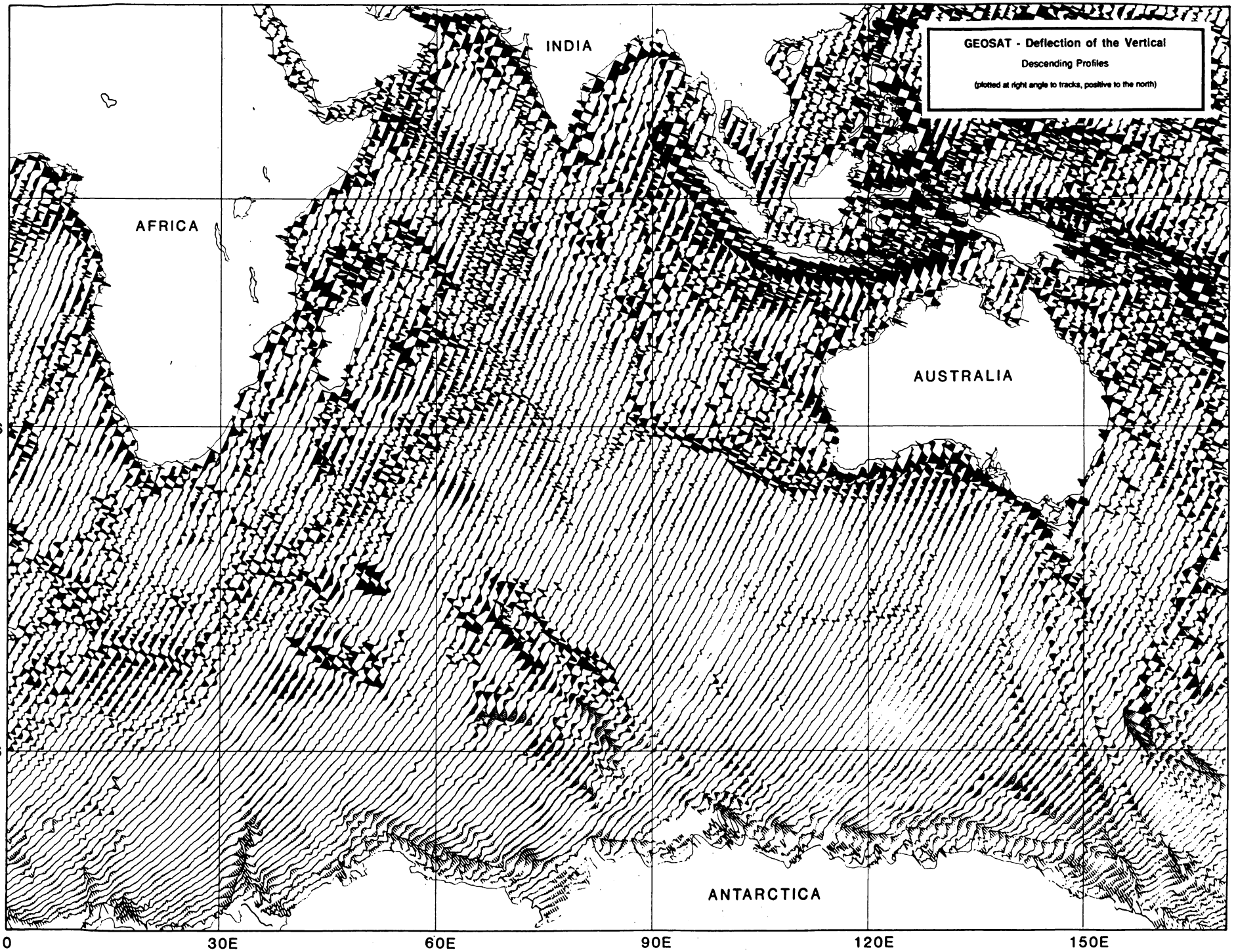

Figure 2

Figure 2

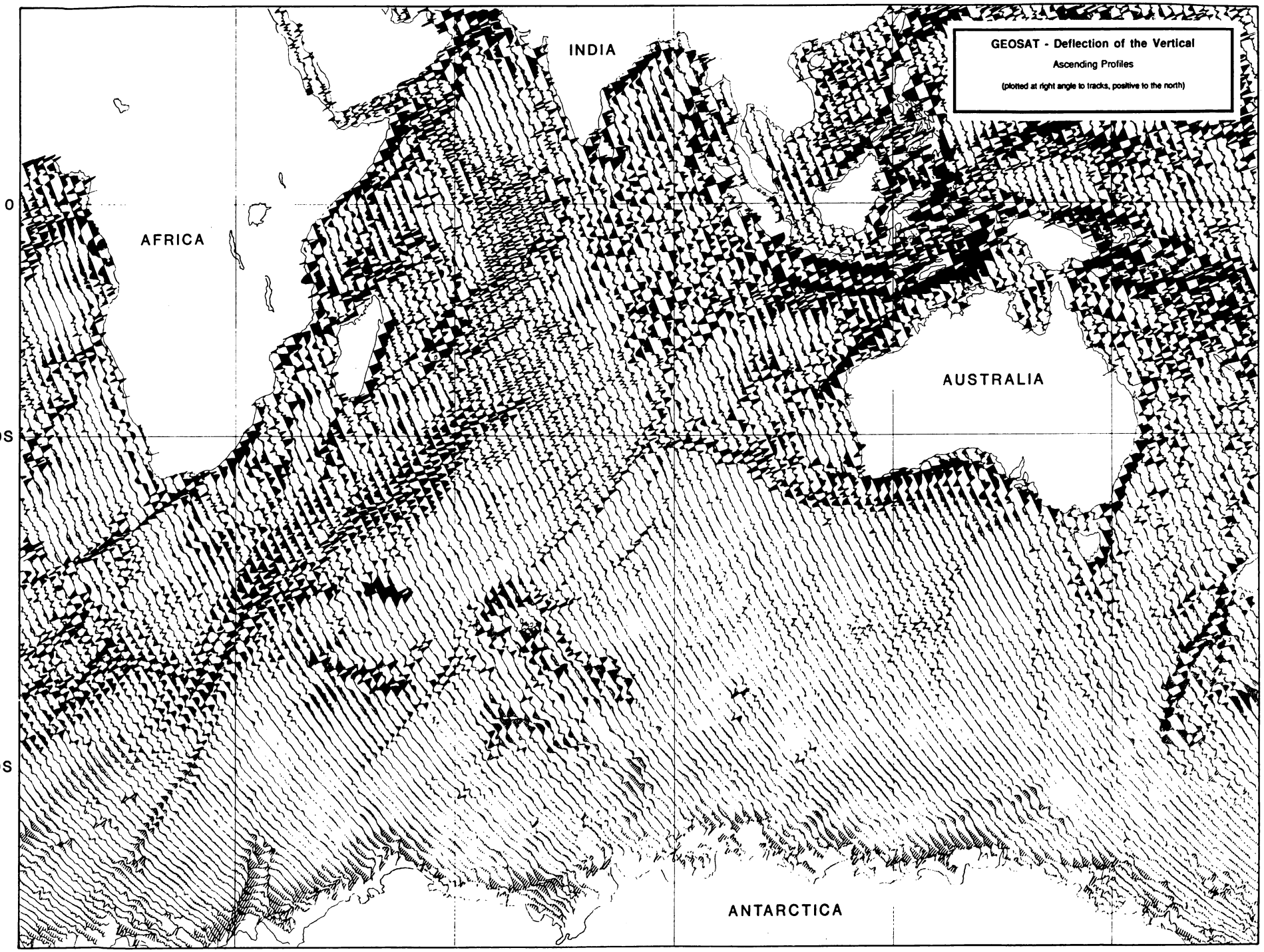

Figure 3

Figure 3

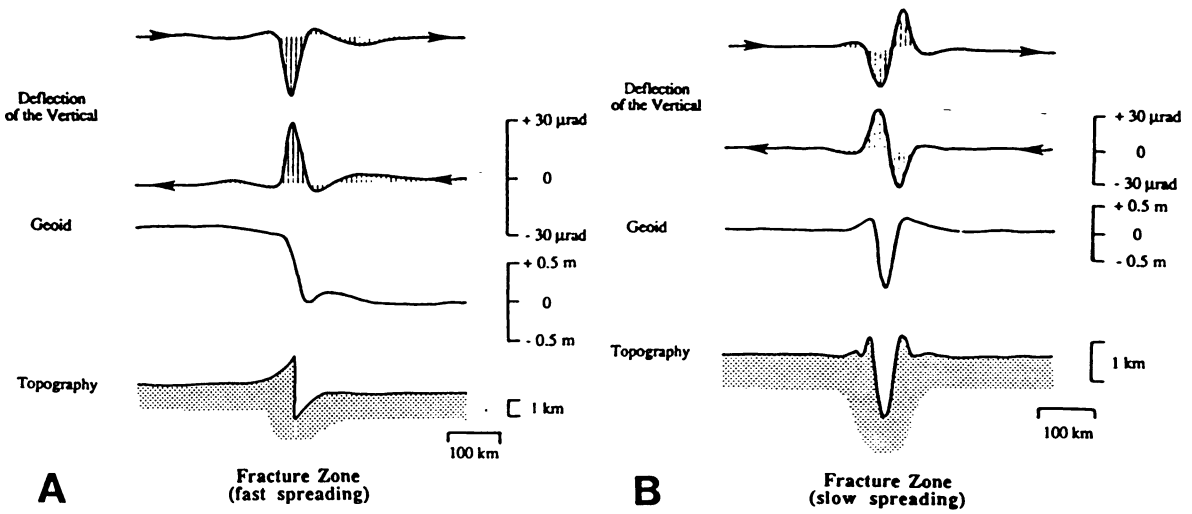
Deflection of the Vertical
+ 30 µrad
0
- 30 µrad
Geoid
+ 0.5 m
0
- 0.5 m
Topography
1 km
100 km
A
Fracture Zone (fast spreading)
Deflection of the Vertical
+ 30 µrad
0
- 30 µrad
Geoid
+ 0.5 m
0
- 0.5 m
Topography
1 km
100 km
B
Fracture Zone (slow spreading)

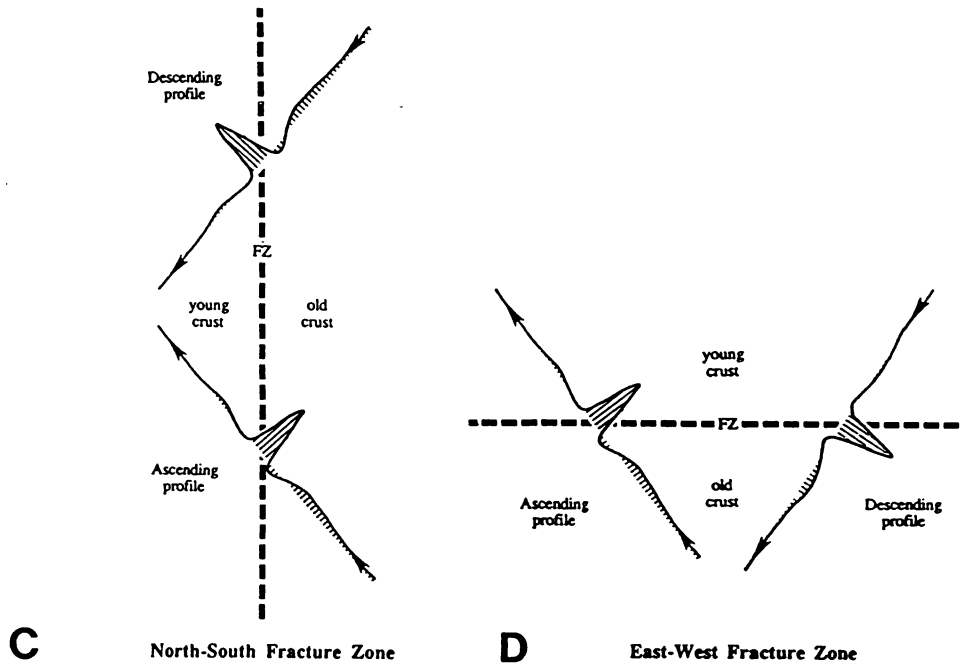
Descending profile
FZ
young crust
old crust
Ascending profile
C
North-South Fracture Zone
young crust
FZ
Ascending profile
old crust
Descending profile
D
East-West Fracture Zone

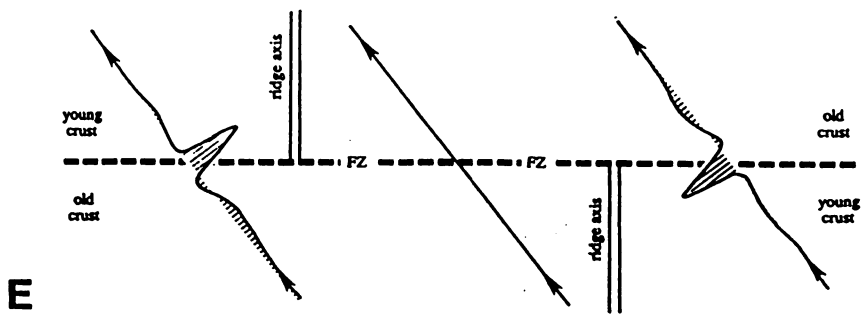
ridge axis
young crust
old crust
FZ
FZ
ridge axis
old crust
young crust
E

Figure 4

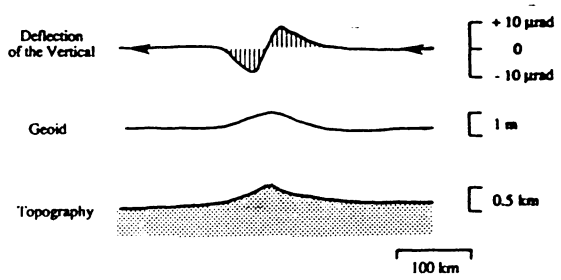

F Spreading Ridge (fast spreading)

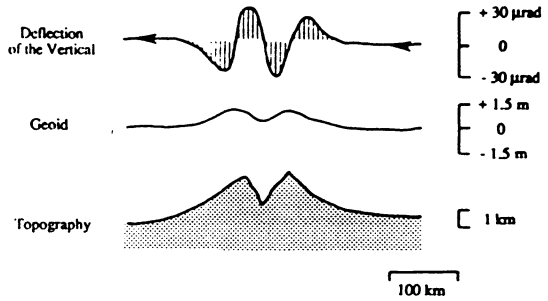

G Spreading Ridge (slow spreading)

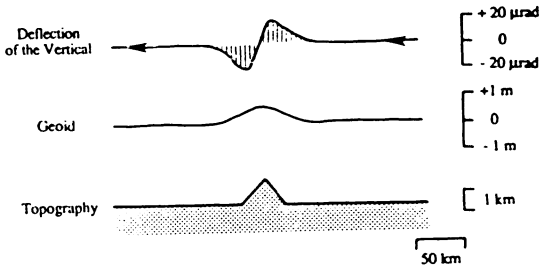

H Seamount

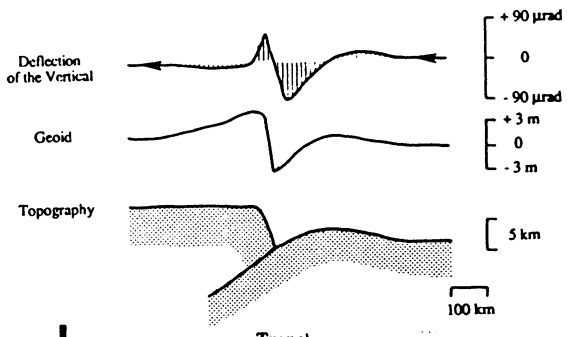

I Trench

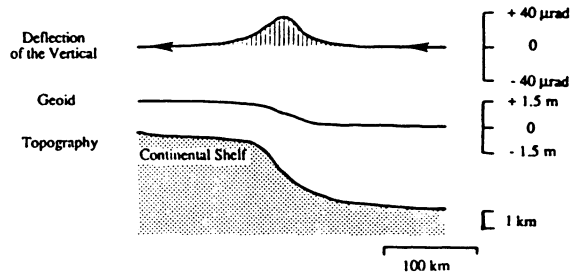

J Continental Slope

Figure 4
(continued)

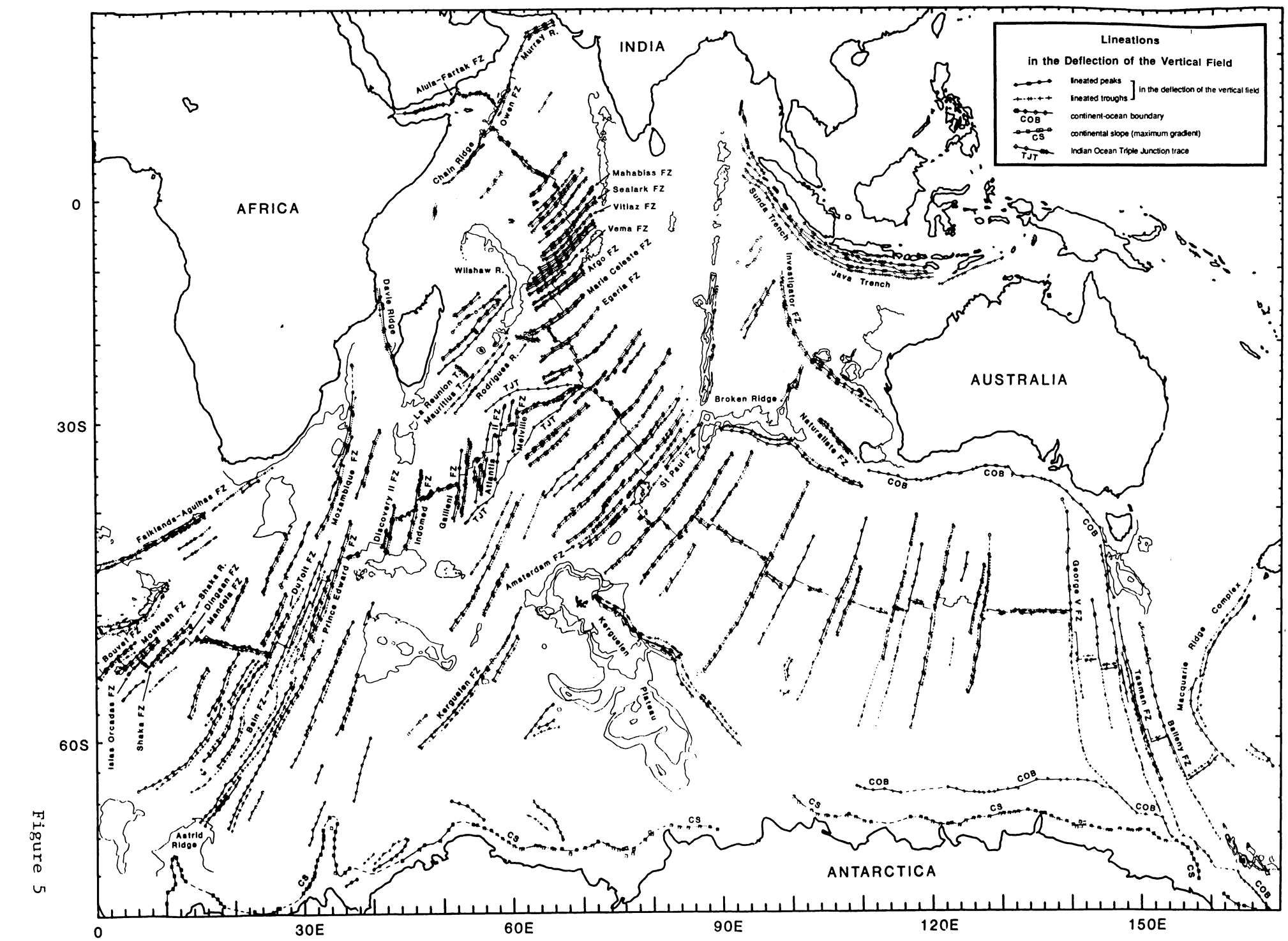

Figure 5

Figure 5

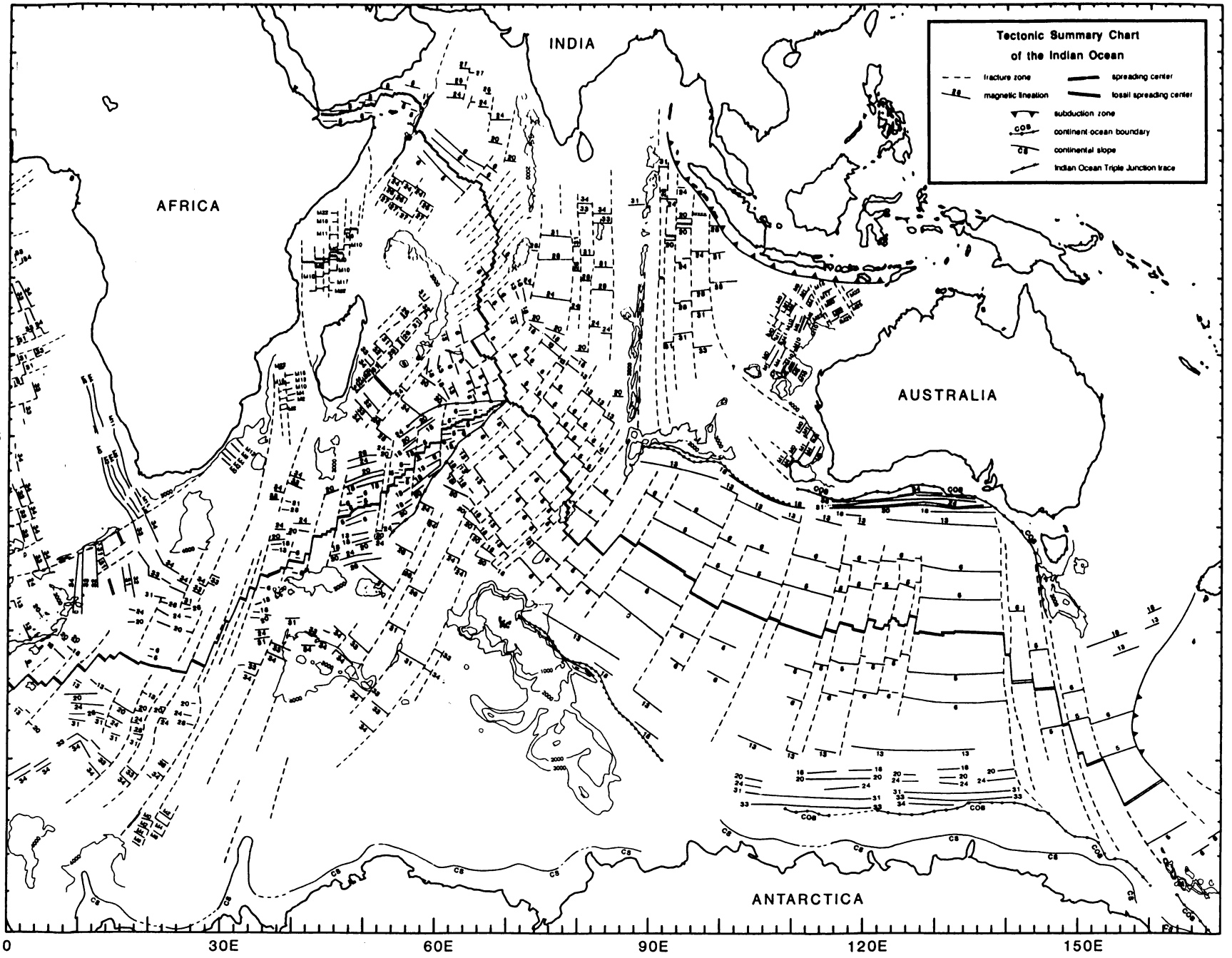

Figure 6
(reduced copy)

Figure 6
(reduced copy)